Theoretical analysis of array-enhanced stochastic resonance in the diffusively coupled FitzHugh-Nagumo equation

Takashi Kanamaru

Department of Electrical and Electronic Engineering,

Tokyo University of Agriculture and Technology, Tokyo 184-8588, Japan

Takehiko Horita

Department of Mathematical Engineering and Information Physics,

The University of Tokyo, Tokyo 113-8656, Japan

Yoichi Okabe

RCAST, The University of Tokyo, Tokyo 153-8904, Japan

Abstract

The array-enhanced stochastic resonance (AESR) in the diffusively coupled FitzHugh-Nagumo equation is investigated. The two properties of AESR, namely, the scaling of the optimal noise intensity and the enhancement of the maximum value of the correlation coefficient as a function of the coupling strength, are analyzed theoretically. By transforming the dynamics of N elements into that of the mean and the deviation from it, it is found that AESR is caused by the correlation between them. A low-dimensional model which reproduces the above properties is constructed.

Physical Review E **64** (2001) 031908.

PACS numbers: PACS numbers: 87.10.+e, 05.45.−a, 84.35.+i, 07.05.Mh

I. INTRODUCTION

In noisy nonlinear systems, stochastic resonance (SR) is a well-known phenomenon where a weak periodic signal is enhanced by its background noise and observed in many systems, such as bistable ring lasers, semiconductor devices, chemical reactions, and neural systems (for reviews, see Refs. [1–4]). When a periodic signal and noise are injected to such systems simultaneously, the signal to noise ratio (SNR) of the output signal is maximized at an optimal noise intensity.

Generally, the neural system has several sources of fluctuations. Firstly, the receptor cells in sensory systems [5] receive signals from the outer world, thus they are exposed to the fluctuations of the environment. Secondly, the ion channels on the membrane of neurons are known to be stochastic [6]. Thirdly, in the central nervous system such as the hippocampus and the cortex, the synaptic transmission is less reliable than that of the peripheral nervous system such as the neuromuscler junction [7–9]. Fourthly, in the cortex, the sum of synaptic inputs from the presynaptic neurons can work as the fluctuation [10–14]. Lastly, chaos in the neural system [15–17] might work as fluctuations in the system. Thus SR may play a significant role in the neural system.

The theoretical works on SR in a single neuron are performed on the integrate-and-fire model [18], the leaky integrate-and-fire model [19, 20], the FitzHugh-Nagumo model [21–23], and the Hodgkin-Huxley model [24]. In those works, it is observed that the output SNR [22, 24] or the peak height of the interspike interval distribution [18–21] takes a maximum as a function of the noise intensity. Some physiological experiments reinforce the hypothesis that the neural system utilizes SR to detect weak signals [25–29]. In Ref. [25], sinusoidally stimulated mechanoreceptor cells of a crayfish with additive noise show the property of SR, namely, the existence of the optimal noise intensity which maximizes the output SNR. In Ref. [26], SR is observed in caudal photoreceptor interneurons of a crayfish by intrinsic and not external noise.

SR in spatially extended systems is also investigated and some new features are demonstrated [30–35]. In Ref. [31], the dependence of the normalized power norm, which measures the correlation between the aperiodic input and the output of the system, on the noise intensity by increasing the number of neurons composing the system is investigated.

In some nonlinear systems [36–38], the correlation between the input and the output takes

a maximum as a function of not only the noise intensity but also the coupling strength, and such a phenomenon is called array-enhanced stochastic resonance (AESR). The term AESR is introduced by Linder et al. [37] to describe the enhancement of the output SNR of a chain of periodically driven damped oscillators, and they found that the degree of synchronization of the elements is also maximized when the output SNR is optimized. Similar phenomenon is also observed in a circuit of diode resonators [38].

Though the above researches treat only the system with periodic inputs, it is known that the coupling of the elements also enhances the "coherence" and the degree of synchronization of the elements in the system without common periodic signals, and this phenomenon is called array-enhanced coherence resonance [39]. Thus the array-enhancement is thought to be a universal phenomenon independent of the input.

In the present paper, we consider the mechanism of AESR in the diffusively coupled FitzHugh-Nagumo model. In Sec. II, the properties of AESR, namely, the scaling of the optimal noise intensity in the strong coupling limit, and the enhancement of the correlation between the input and the output caused by the coupling, are introduced. In Secs. III and IV, we transform the dynamics of the network of N neurons into that of the mean and the deviation $\delta x^{(i)}$, and construct the models which describe AESR. It is found that AESR is caused by the correlation between the mean X and the deviation $\delta x^{(i)}$. In Sec. V, the validity of the approximation is examined, and it is found that the nonlinear effect cannot be neglected for large N. Conclusions and discussions are given in the final section.

II. AESR IN THE DIFFUSIVELY COUPLED FN MODEL

In the present paper, we treat the diffusively coupled FitzHugh-Nagumo (FN) model written by

$$\tau \frac{du_i}{dt} = -v_i + u_i - \frac{u_i^3}{3} + S(f;t) + \eta_i(t) + \frac{w}{N}\sum_{j=1}^{N}(u_j - u_i), \tag{1}$$

$$\frac{dv_i}{dt} = u_i - \beta v_i + \gamma, \tag{2}$$

$$S(f;t) = \begin{cases} S_0 & \text{if } n/f \le t \le n/f + h \ \ (n = 0, 1, 2, \cdots), \\ 0 & \text{otherwise,} \end{cases} \tag{3}$$

$$\langle \eta_i(t)\eta_j(t')\rangle = D\delta_{ij}\delta(t - t'), \tag{4}$$

for $i = 1, 2, \cdots, N$, where β, γ, and τ are system parameters of the elements, u_i is the variable which models the membrane potential of the i-th neuron, v_i is the variable which represents the refractoriness after the firing of the i-th neuron, $S(f;t)$ is a periodic pulse train with height S_0, width h, and frequency f, $\eta_i(t)$ is Gaussian white noise with intensity D which models the fluctuations in the system, and δ_{ij} denotes Kronecker's delta. Note that the connection of the elements is diffusive, the periodic pulse train $S(f;t)$ is applied to all the elements, and noises for different elements are statistically independent.

A single FN model shows a characteristic of an excitable system, namely, it has a stable rest state $u_i \simeq -1.2$, and with an appropriate amount of disturbance it generates a pulse with a characteristic magnitude of height and width. When u_i takes a larger value than 1, we call that the system generates an output pulse. In the following, parameter values $\beta = 0.8$, $\gamma = 0.7$, $\tau = 0.1$, $S_0 = 0.1$, $f = 0.5$, and $h = 0.3$, are used. Note that the input pulse height S_0 is so small that the system does not generate any output pulse without a certain amount of noise, namely, the input pulse is sub-threshold.

By the symmetry of the system, the behaviors of all the elements are statistically identical, and we regard the internal state $u_1(t)$ of the first element as the output of the system. To measure the correlation between the input $S(f;t)$ and the output $u_1(t)$, let us define the correlation coefficient C between the input and output pulse trains [40]. To incorporate the effect of the firing delay d_f of the FN model, which is the time lag of the firing since an input pulse is injected, the shift $t \to t - d_f$ is applied to the time series of the output pulse train. After the shift of t, the time interval under observation is divided into n bins of the width Δ, and the number of pulses in the i-th bin is denoted as X_i and Y_i for the input and output pulses, respectively. Note that the width Δ is sufficiently small so that X_i and Y_i take the value 0 or 1. Then $X = \sum X_i$ and $Y = \sum Y_i$ are the numbers of input and output pulses respectively, and $Z = \sum X_i Y_i$ is the number of coincident pulses. The correlation coefficient C between the input and output pulse trains is defined as

$$C = \frac{Z - (XY)/n}{\sqrt{X(1 - X/n)Y(1 - Y/n)}} \in [-1, 1]. \tag{5}$$

Consider the periodic input pulse train with frequency f, then

$$X_i = \begin{cases} 1 & \text{for every } (1/\Delta f)\text{-th bins,} \\ 0 & \text{otherwise.} \end{cases} \tag{6}$$

If the output sequence Y_i is identical with X_i, namely, if the relation $X_i = Y_i$ is satisfied for all i, the correlation coefficient C takes the value 1. If the output series Y_i has no correlation with X_i, the correlation coefficient C takes the value 0 in the large n limit. We set $\Delta = 0.5$ in the following.

The dependence of the correlation coefficient C on the noise intensity D for $w = 0$, 0.5, 1.0, and 2.0 with $N = 10$ is shown in Fig. 1. The data for each w shows the typical property

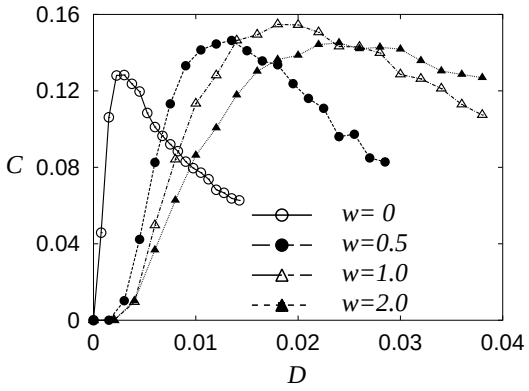

FIG. 1: The dependence of the correlation coefficient C on the noise intensity D for $w = 0$, 0.5, 1.0, and 2.0 with $N = 10$.

of stochastic resonance, namely, the existence of a peak of the correlation coefficient C as a function of the noise intensity D. It is also observed that the optimal noise intensity D_0 increases with the increase of the coupling strength w, and the maximum value C_{peak} of C at $D = D_0$ also depends on w.

The dependence of the optimal noise intensity D_0 on the coupling strength w for $N = 10$, 50, and 100 is shown in Fig. 2. For large w, it is observed that D_0 converges to a value dependent on the number N of neurons. As shown in the next section, the asymptotic value $D_0^{(N)}(\infty)$ of the optimal noise intensity for the network of N neurons satisfies

$$D_0^{(N)}(\infty) = N D_0^{(1)}(\infty). \tag{7}$$

The dependence of C_{peak} on the coupling strength w for $N = 10$, 50, and 100 is shown in Fig. 3, and it is observed that C_{peak} takes a maximum as a function of w. This phenomenon where the correlation between the input and the output takes a maximum as a function of not only the noise intensity but also the coupling strength is called array-enhanced stochastic resonance (AESR) and observed in some nonlinear systems [36–38].

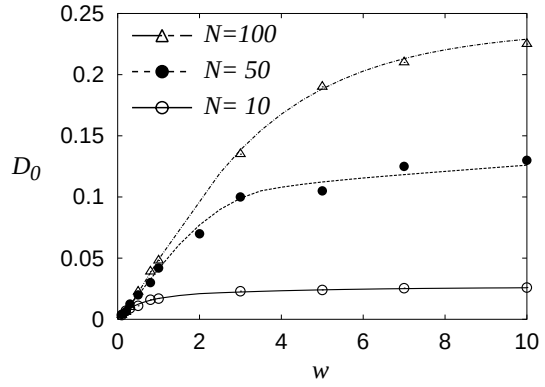

FIG. 2: The dependence of the optimal noise intensity D_0 on the coupling strength w for $N = 10$, 50, and 100.

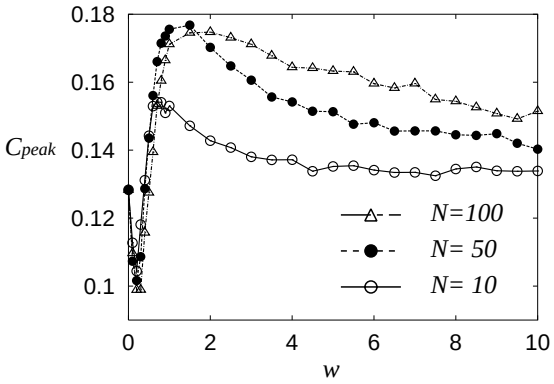

FIG. 3: The dependence of the maximum value C_{peak} of the correlation coefficient C on the coupling strength w for $N = 10$, 50, and 100.

In the following sections, we analyze the mechanism of AESR in the diffusively coupled FitzHugh-Nagumo model.

III. MODEL OF AESR: APPROXIMATION 1

To analyze the mechanism of AESR, the dynamics of the coupled FN model composed of N neurons is rewritten as

$$\frac{dx^{(i)}}{dt} = F(x^{(i)}) + \frac{w}{\tau} A \left(X - x^{(i)} \right) + \frac{1}{\tau} \eta^{(i)}, \tag{8}$$

$$X = \frac{1}{N} \sum_{i=1}^{N} x^{(i)}, \tag{9}$$

$$\langle \eta_i(t)\eta_j(t')\rangle = D\delta_{ij}\delta(t-t'), \tag{10}$$
$$i,j = 1,2,\cdots,N,$$

where $x^{(i)} = (x_1^{(i)}, x_2^{(i)})^t = (u_i, v_i)^t$, $\eta^{(i)} = (\eta_i, 0)^t$, and A is a two dimensional diagonal matrix with diagonal components $A_1 = 1$ and $A_2 = 0$. Note that $F(x^{(i)}) = (F_1(x^{(i)}), F_2(x^{(i)}))^t$ with

$$F_1(x^{(i)}) = \frac{1}{\tau}\left(-v_i + u_i - \frac{u_i^3}{3} + S(f;t)\right), \tag{11}$$
$$F_2(x^{(i)}) = u_i - \beta v_i + \gamma, \tag{12}$$

denotes the internal motion of the i-th neuron. Let us define the deviation $\delta x^{(i)}$ of the i-th neuron from the mean X as

$$\delta x^{(i)} = x^{(i)} - X. \tag{13}$$

The variables X and $\delta x^{(i)}$ obey

$$\frac{dX}{dt} = F(X) + \frac{1}{\tau N}\sum_{i=1}^{N}\eta^{(i)} + \epsilon, \tag{14}$$
$$\frac{d}{dt}\delta x^{(i)} = \left(DF(X) - \frac{w}{\tau}A\right)\delta x^{(i)} + \frac{1}{\tau}\left(\eta^{(i)} - \frac{1}{N}\sum_{j=1}^{N}\eta^{(j)}\right) + \xi^{(i)} - \epsilon, \tag{15}$$

where $DF(x)$ is the Jacobian matrix of $F(x)$ and

$$\epsilon \equiv \frac{1}{N}\sum_{i=1}^{N}F(X+\delta x^{(i)}) - F(X) \tag{16}$$

and

$$\xi^{(i)} \equiv F(X+\delta x^{(i)}) - \left(F(X) + DF(X)\delta x^{(i)}\right) \tag{17}$$

are $O(|\delta x^{(i)}|^2)$. Since F_2 is a linear function and $\sum_{i=1}^{N}\delta x^{(i)} = 0$, the nonlinear terms ϵ and $\xi^{(i)}$ can be expressed as $(\epsilon, 0)^t$ and $(\xi^{(i)}, 0)^t$, respectively.

For sufficiently large w, with the approximation $\xi^{(i)} = \epsilon = 0$, Eq. (15) becomes

$$\frac{d}{dt}\delta x_1^{(i)} = -\frac{1}{\tau}(w - 1 + X_1^2)\delta x_1^{(i)} - \frac{1}{\tau}\delta x_2^{(i)} + \frac{1}{\tau}\left(\eta_i - \frac{1}{N}\sum_{j=1}^{N}\eta_j\right), \tag{18}$$
$$\frac{d}{dt}\delta x_2^{(i)} = \delta x_1^{(i)} - \beta\delta x_2^{(i)}, \tag{19}$$

where β is the parameter of the FN model. As shown in Appendix A, the variance of $\delta x_1^{(i)}$ is estimated to be

$$\langle(\delta x_1^{(i)})^2\rangle \simeq \frac{(1-N^{-1})D}{2\tau(w-1+X_1^2)}, \tag{20}$$

which justifies the approximation to neglect the nonlinear terms

$$\xi^{(i)} = -\frac{1}{\tau}\left(X_1(\delta x_1^{(i)})^2 + \frac{(\delta x_1^{(i)})^3}{3}\right) \tag{21}$$

and

$$\epsilon = -\frac{1}{\tau N}\sum_{i=1}^{N}\left(X_1(\delta x_1^{(i)})^2 + \frac{(\delta x_1^{(i)})^3}{3}\right) \tag{22}$$

in Eq. (15) for large w and thus, in the large w limit, the mean dynamics of X approaches to the dynamics of the single neuron, i.e., the dynamics governed by Eq. (14) with $\epsilon = 0$. Note that Eq. (14) with $\epsilon = 0$ justifies the scaling of the asymptotic value of the optimal noise intensity (Eq. (7)).

To analyze AESR, let us take the quadratic term in Eq. (14) into consideration by ignoring higher order terms, i.e., we consider Eq. (14) with

$$\epsilon \simeq -\frac{X_1}{\tau N}\sum_{i=1}^{N}(\delta x_1^{(i)})^2, \tag{23}$$

$$= -\frac{1}{\tau}X_1(\delta x_1)^2, \tag{24}$$

where

$$(\delta x_1)^2 \equiv \frac{1}{N}\sum_{i=1}^{N}(\delta x_1^{(i)})^2. \tag{25}$$

As shown in Appendix B, for large N, $(\delta x_1)^2$ is approximated by

$$(\delta x_1)^2 \simeq \langle(\delta x_1^{(i)})^2\rangle. \tag{26}$$

Note that with the same accuracy of approximation $(1/N)\sum(\delta x_1^{(i)})^3 \simeq 0$ which also supports the approximation (23). For large enough w, Eq. (26) with Eq. (20) is approximated by

$$(\delta x_1)^2 \simeq \frac{(1-N^{-1})D}{2\tau w}, \tag{27}$$

which is a constant independent of t and denoted by $(\delta x_1)^2_{app1}$ in the following.

The time series of $(\delta x_1)^2$ and X_1 constructed from the numerical solutions of $x_1^{(i)}$ for $N = 50$, $w = 10$, and $D = 0.125$ are shown in Fig. 4. Although it is observed that $(\delta x_1)^2$ largely fluctuates around its mean value, it may be plausible to compare the long time average

$$\overline{(\delta x_1)^2} \equiv \lim_{T\to\infty}\frac{1}{T}\int_0^T(\delta x_1)^2 dt. \tag{28}$$

of $(\delta x_1)^2$ with $(\delta x_1)^2_{app1}$. In Fig. 5, $(\delta x_1)^2_{app1}$ and $\overline{(\delta x_1)^2}$ for $N = 10$ and 50 along the curves

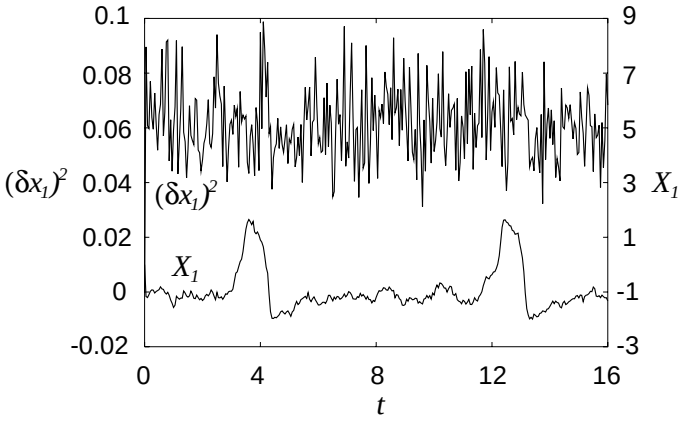

FIG. 4: The time series of $(\delta x_1)^2$ and X_1 for $N = 50$, $w = 10$, and $D = 0.125$.

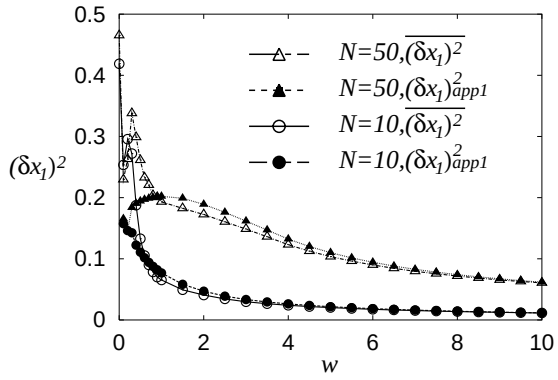

FIG. 5: The values of $(\delta x_1)^2_{app1}$ and $\overline{(\delta x_1)^2}$ for $N = 10$ and 50 along the curves in $w - D$ plane in Fig. 2 are plotted against w.

in $w - D$ plane in Fig. 2 are plotted against w. It is observed that $(\delta x_1)^2_{app1}$ well describes the behavior of $\overline{(\delta x_1)^2}$ for large w.

Based on the above discussions, let us describe the mean dynamics X by

$$\frac{dX}{dt} = F(X) + \frac{1}{\tau}\hat{\eta} + \epsilon, \tag{29}$$

$$\hat{\eta} \equiv (\hat{\eta}, 0)^t, \tag{30}$$

$$\epsilon \equiv \left(-\frac{1}{\tau}X_1\overline{(\delta x_1)^2}, 0\right)^t, \tag{31}$$

$$\langle\hat{\eta}(t)\hat{\eta}(t')\rangle = \frac{D}{N}\delta(t - t'). \tag{32}$$

Note that this model is derived by substituting the constant value $\overline{(\delta x_1)^2}$ for $(\delta x_1)^2$ in Eq. (24). In the following, the system governed by Eqs. (29) and (31) is called as the

approximation 1. The numerical simulations of the approximation 1 are performed as follows:

- Fix a set of values of w and D on the curve in the $w - D$ plane in Fig. 2;
- Numerically obtain the value of $\overline{(\delta x_1)^2}$ for the network of N neurons with the above fixed w and D;
- Obtain the correlation coefficient C of X_1 for the approximation 1 with the above D and $\overline{(\delta x_1)^2}$.

The dependences of the peak values C_{peak}'s of the correlation coefficient C on the coupling strength w of the approximation 1 and the network of N neurons are compared in Fig. 6. It

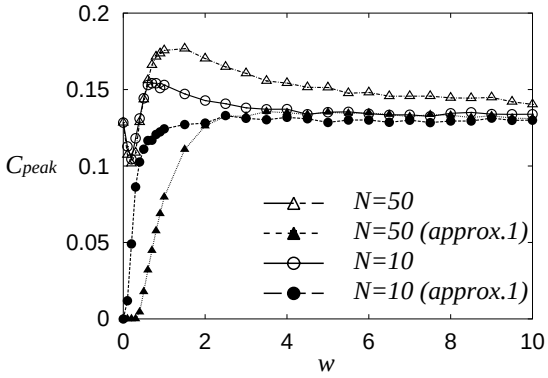

FIG. 6: The dependences of the peak values C_{peak}'s of the correlation coefficient C on the coupling strength w of the approximation 1 and the network of N neurons.

is observed that the approximation 1 does not show the enhancement of C_{peak}, namely, C_{peak} of the approximation 1 always takes smaller values than that of the single neuron ~ 0.13. In other words, the quadratic term $(\delta x_1)^2$ modeled by the constant $\overline{(\delta x_1)^2}$ cannot reproduce the properties of AESR. This suggests that the time dependence of $(\delta x_1)^2$ is important for the enhancement of stochastic resonance.

In the next section, we take the time dependence of $(\delta x_1)^2$ into consideration by retrieving the mean X_1 in $\langle (\delta x_1^{(i)})^2 \rangle$.

IV. MODEL OF AESR: APPROXIMATION 2

In this section, the approximation of $(\delta x_1)^2$ by

$$(\delta x_1)^2_{app2} = \frac{(1 - N^{-1})D}{2\tau(w - 1 + X_1^2)} \tag{33}$$

is considered according to Eqs. (20) and (26). Note that Eq. (33) is valid only for $w \gg 1$ as shown in Appendix A and at least w must be greater than 1 in order that the denominator does not vanish.

Let us consider the approximation 2 governed by Eq. (29) with

$$\epsilon \equiv \left(-\frac{1}{\tau} X_1 (\delta x_1)^2_{app2}, 0 \right)^t . \tag{34}$$

The dependences of C_{peak}'s in both the approximation 2 and the network of N neurons on w are shown in Fig. 7. It is observed that the enhancement of C_{peak} for $w > 0$ is qualitatively

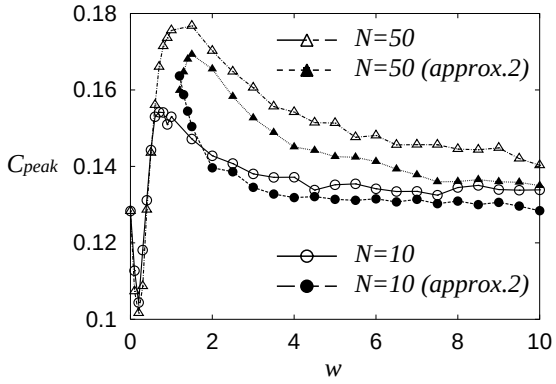

FIG. 7: The dependences of C_{peak}'s of the approximation 2 and network of N neurons on w.

described by the approximation 2.

From the above discussions, it can be concluded that AESR is caused by the dependence of the term $(\delta x_1)^2$ on the mean X_1 of N neurons. Compared with the single neuron case, which is also realized by Eqs. (29), (33), and (34) in the large w limit, the modification of the system by ϵ is considered to make the system to fire more easily, i.e., the modification lowers the threshold of firing of the system. The noise intensity is adjusted for the change of w according to Fig. 2, thus the noise intensity applied to the system with $w \simeq 1.5$ is smaller than that for the single neuron ($w \gg 1$). Since the threshold of firing is lowered, the relatively small noise enables the system to fire more coherently correlated with the periodic input and brings an enhancement of C.

Meanwhile, as shown in Fig. 7, C_{peak} of the approximation 2 still underestimates that of the network of N neurons, and the deviation seems to grow for large N. In the next section, we consider this effect and examine the validity of the above approximation.

V. VALIDITY OF THE APPROXIMATION

In the above analyses, we used two approximations, namely, the linearization of the dynamics of $\delta x^{(i)}$ (Eqs. (18) and (19)), and the neglect of the fluctuation of $(\delta x_1)^2$ (Eq. (26)). In this section, we examine the validity of these approximations.

First, we examine the validity of the linearization by investigating the magnitude of $(\delta x_1)^2$ at the several points shown in Fig. 8. Three curves in Fig. 8 show the optimal noise intensity

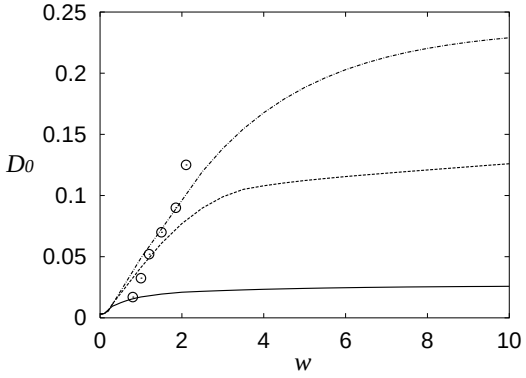

FIG. 8: The location (w_0, D_0^*) of the maximum of C_{peak} where C attains its maximum as a function of both D and w for several fixed values of N. Three curves show the optimal noise intensity D_0 as a function of w for $N = 10$, 50, and 100.

D_0 as a function of w for three fixed N, and the circles indicate the location (w_0, D_0^*) of the maximum of C_{peak} where C attains its maximum as a function of both D and w for several fixed values of N (see also Fig. 3). Our concern is the validity of the linear approximation for D and w around D_0^* and w_0. In Fig. 9, $\overline{(\delta x_1)^2}$ with D_0^* and w_0 is plotted against N, and it is observed that $\overline{(\delta x_1)^2}$ increases with the increase of N with a power law $\sim N^{0.5}$ in this range of N. This behavior of $\overline{(\delta x_1)^2}$ is understood as follows. Since the system is driven by Gaussian white noise, if w is fixed, $\overline{(\delta x_1)^2}$ increases with D and $\overline{(\delta x_1)^2} \to \infty$ as $D \to \infty$. On the other hand, the coupling of the elements suppresses the fluctuation of the elements as in Eq. (33), and the balance between D and w controls the magnitude of $\overline{(\delta x_1)^2}$. In the range of N considered in Fig. 9, D_0^* grows faster than the growth of w_0 with N and the dependence $\overline{(\delta x_1)^2} \sim N^{0.5}$ is observed. This dependence of $\overline{(\delta x_1)^2}$ on N is expected to hold for large N until its magnitude becomes large such that the nonlinear terms in Eq. (15) cannot be neglected and the linear approximation in Eq. (18) cannot hold. Thus, for large

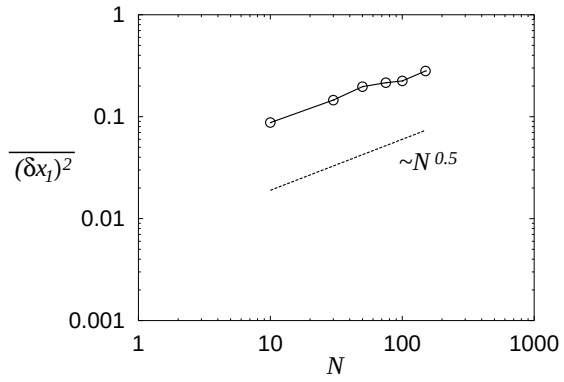

FIG. 9: $\overline{(\delta x_1)^2}$ against N at the points shown in Fig. 8.

N, the linear approximation shall not be valid.

Next, let us consider the effect of the deviation of $(\delta x_1)^2$ from $(\delta x_1)^2_{app2}$, i.e., the fluctuations of $(\delta x_1)^2$ under the assumption that the linear approximation in Eq. (18) is valid. If the fluctuations of $(\delta x_1)^2$ cause the deviation of the approximation 2 from the network of N neurons, they must enhance C_{peak} of the approximation 2 as shown in Fig. 7.

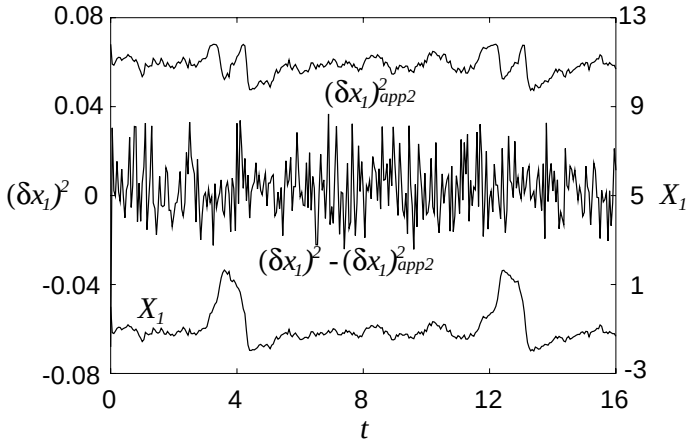

FIG. 10: The time series of the fluctuations of $(\delta x_1)^2$ for $N = 50$, $w = 10$, and $D = 0.125$. The time series of X_1 and $(\delta x_1)^2_{app2}$ are also shown.

The time series of the fluctuations of $(\delta x_1)^2$ is shown in Fig. 10, and it is observed that the fluctuations have large intensity and cannot be neglected in comparison with $(\delta x_1)^2_{app2}$. The probability density function of the fluctuations of $(\delta x_1)^2$ is shown in Fig. 11. As shown

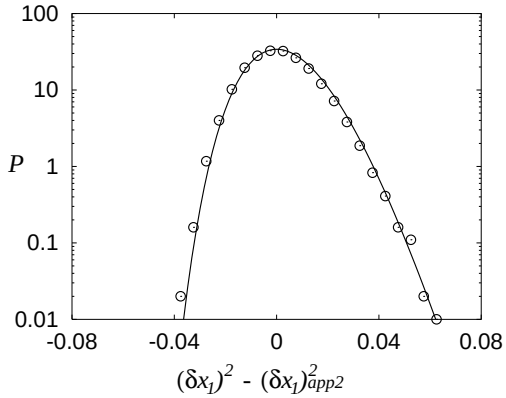

FIG. 11: The distribution of the fluctuations of $(\delta x_1)^2$.

in Appendix B, $(\delta x_1)^2$ obeys the distribution

$$P_2(y;t) \propto \exp\left[-\frac{N-1}{2\langle(\delta x_1)^2\rangle}\left(y - \frac{N-3}{N-1}\langle(\delta x_1)^2\rangle \log y\right)\right] \tag{35}$$

for large N. The fitting with Eq. (35) with a constant instead of time dependent $\langle(\delta x_1)^2\rangle$ is in good agreement with the empirical distribution. It is also observed that the distribution is highly asymmetric, thus the fluctuations of $(\delta x_1)^2$ tend to take large positive values. Note that the large positive fluctuations of $(\delta x_1)^2$ help the mean X_1 to fire because the term $\propto -X_1(\delta x_1)^2$ in Eq. (24) gives the positive influences to $X_1(< 0)$ in the equilibrium.

Furthermore, as shown in Appendix B, the variance of $(\delta x_1)^2$ is written as

$$\langle((\delta x_1)^2 - \langle(\delta x_1)^2\rangle)^2\rangle \simeq \frac{2}{N-1}\langle(\delta x_1^{(i)})^2\rangle^2. \tag{36}$$

Equation (36) indicates that the magnitude of the fluctuations of $(\delta x_1)^2$ depends on $\langle(\delta x_1^{(i)})^2\rangle$ and X_1. It may be plausible to consider that the asymmetrically distributed fluctuations with the amplitude depending on X_1 enhances C and this may be one of the reasons for the discrepancy between the approximation 2 and the full system. Moreover, the scaling $\langle(\delta x_1^{(i)})^2\rangle \sim N^{0.5}$ and Eq. (36) indicate that the fluctuations of $(\delta x_1)^2$ does not decay with N, thus the fluctuations can not be neglected even if they are small compared with $\langle(\delta x_1)^2\rangle$.

From the above discussions, it is found that neither the linearization of the dynamics of $\delta x^{(i)}$ nor the neglect of the fluctuation of $(\delta x_1)^2$ are valid for large N. To construct more precise theories for AESR, the effects of nonlinear terms and the fluctuations must be considered.

VI. CONCLUSIONS AND DISCUSSIONS

The array-enhanced stochastic resonance (AESR) in the diffusively coupled FitzHugh-Nagumo model is investigated. AESR is characterized by the following two properties, namely, the scaling of the optimal noise intensity $D_0^{(N)}(\infty)$ for N neurons with the sufficiently large coupling strength obeying

$$D_0^{(N)}(\infty) = N D_0^{(1)}(\infty), \tag{37}$$

and the enhancement of the maximum value C_{peak} of the correlation coefficient C as a function of the coupling strength w.

By transforming the dynamics of N neurons into that of the mean X and the deviation $\delta x^{(i)}$, it is found that AESR is well described by a reduced dynamics of the mean X, particularly by the correlation between $(\delta x_1)^2$ and X_1.

The validity of the approximation is examined, and it is found that neither the linearization of the dynamics of $\delta x^{(i)}$ nor the neglect of the fluctuation of $(\delta x_1)^2$ are valid for large N. To construct more precise theories for AESR, the effects of nonlinear terms and the fluctuations must be considered.

Note that our analyses are independent of the input, thus the above discussions are also applicable to the array-enhancement in the system without the input, namely, array-enhanced coherence resonance [39].

As for the information processing in the neural system, AESR gives a mechanism for an effective regulation of the noise intensity even for the "uncontrollable" noises. As shown in Fig. 12(a), the regulation of the noise intensity in the $w-D$ plane is represented by a vertical arrow, and the dependence of the correlation coefficient C on the noise intensity D along this arrow is shown in Fig. 1. Note that the correlation coefficient C takes a maximum when the arrow crosses the curve which shows the optimal noise intensity. On the other hand, a horizontal arrow in Fig. 12(a) represents the regulation of the coupling strength, and the dependence of C on the coupling strength w along this arrow is shown in Fig. 12(b). It is shown that the correlation coefficient takes a maximum when w crosses the curve of optimal noise intensity shown in Fig. 12(a). Thus the regulation of w might work as a mechanism for the effective regulation of the noise intensity even for the "uncontrollable" noises in the neural system.

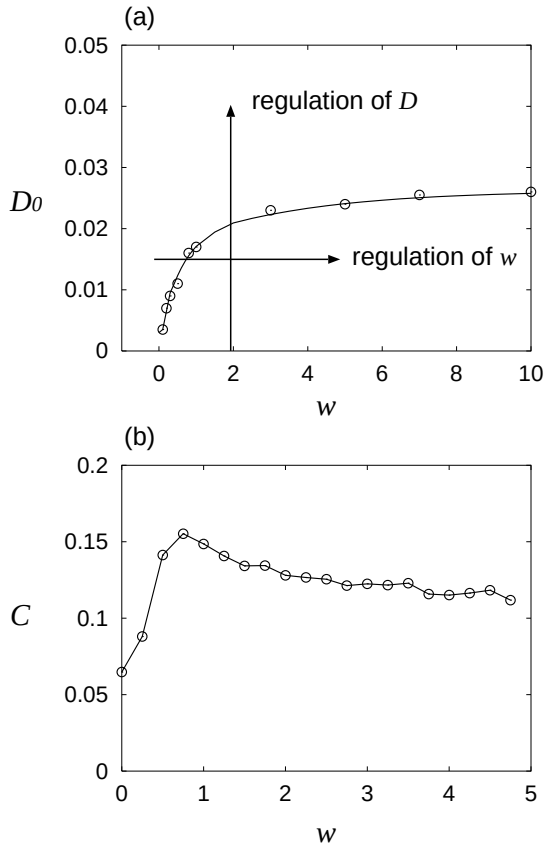

FIG. 12: (a) The dependence of the optimal noise intensity D_0 on the coupling strength w for $N = 10$. (b) The dependence of the correlation coefficient C on the coupling strength w for $D = 0.015$ and $N = 10$.

Acknowledgments

The authors (T.K. and T.H.) are grateful to Professor H. Hata for his stimulating discussion and encouragement. The authors are also grateful to the referee for valuable comments.

APPENDIX A: DERIVATION OF $\langle(\delta x_1^{(i)})^2\rangle$

In this appendix, we analytically derive the term $\langle(\delta x_1^{(i)})^2\rangle$ given by Eq. (20), namely,

$$\langle(\delta x_1)^2\rangle \simeq \frac{(1-N^{-1})D}{2\tau(w-1+X_1^2)}, \tag{A1}$$

from the linearized stochastic differential equation

$$\frac{d}{dt}\delta x_1 \;=\; -\frac{1}{\tau}(w-1+X_1^2)\delta x_1 - \frac{1}{\tau}\delta x_2 + \frac{1}{\tau}\tilde{\eta}, \tag{A2}$$

$$\frac{d}{dt}\delta x_2 = \delta x_1 - \beta \delta x_2, \tag{A3}$$

$$\langle \tilde{\eta}(t)\tilde{\eta}(t')\rangle = (1 - N^{-1})D\delta(t - t'), \tag{A4}$$

where the suffix (i) which denotes the index of the neuron is omitted for simplicity.

With the vector $x = (\delta x_1, \delta x_2)^t$, Eqs. (A2) and (A3) are written as

$$\frac{d}{dt}x = A(t)x + f(t). \tag{A5}$$

Let us denote the solution of $\dot{x} = A(t)x$ as $x(t) = B(t)x(0)$ by the solution matrix $B(t)$. Then, with $B(t,s) \equiv B(t)B^{-1}(s)$, the solution of Eq. (A5) is written as

$$x(t) = B(t,t_0)x(t_0) + \int_{t_0}^{t} ds B(t,s)f(s). \tag{A6}$$

We assume that $B(t,s)$ rapidly converges to 0 as $t - s \to \infty$, which enables us to neglect the nonlinear terms $\xi^{(i)}$ and ϵ in the dynamics of $\delta x^{(i)}$ governed by Eq. (15).

With $\tilde{\eta} = 0$, Eq. (A2) is solved to be

$$\delta x_1(t) = \phi(t,t_0)\delta x_1(t_0) - \frac{1}{\tau}\int_{t_0}^{t} ds \phi(t,s)\delta x_2(s), \tag{A7}$$

where

$$\phi(t,s) \equiv \exp\left[-\frac{1}{\tau}(w-1)(t-s) - \frac{1}{\tau}\int_s^t dt' X_1^2(t')\right]. \tag{A8}$$

The assumption that $B(t,s) \to 0$ as $t - s \to \infty$ requires the condition that $\phi(t,s) \to 0$ as $t - s \to \infty$.

If the convergence of $\phi(t,s)$ to 0 as $t - s \to \infty$ is sufficiently rapid, $\delta x_2(s)$ in Eq. (A7) can be replaced by $\delta x_2(t)$. With this assumption, Eq. (A7) becomes

$$\delta x_1(t) \simeq \phi(t,t_0)\delta x_1(t_0) - \psi(t,t_0)\delta x_2(t), \tag{A9}$$

$$\psi(t,s) \equiv \frac{1}{\tau}\int_s^t dt' \phi(t,t'). \tag{A10}$$

Substituting Eq. (A9) in Eq. (A3), we obtain

$$\frac{d}{dt}\delta x_2 = \phi(t,t_0)\delta x_1(t_0) - (\psi(t,t_0) + \beta)\delta x_2, \tag{A11}$$

and it is solved as

$$\delta x_2(t) = \exp\left[-\int_{t_0}^{t} ds(\psi(s,t_0) + \beta)\right]\delta x_2(t_0) + \int_{t_0}^{t} ds \exp\left[-\int_s^t dt'(\psi(t',t_0) + \beta)\right]\phi(s,t_0)\delta x_1(t_0). \tag{A12}$$

From Eqs. (A9) and (A12), for $t > s$, we obtain

$$B_{21}(t,s) = \int_s^t ds' \exp\left[-\int_{s'}^t dt'(\psi(t',s)+\beta)\right]\phi(s',s), \tag{A13}$$

$$B_{22}(t,s) = \exp\left[-\int_s^t ds'(\psi(s',s)+\beta)\right], \tag{A14}$$

$$B_{11}(t,s) = \phi(t,s) - \psi(t,s)B_{21}(t,s), \tag{A15}$$

$$B_{12}(t,s) = -\psi(t,s)B_{22}(t,s). \tag{A16}$$

With the assumption that the convergence of $\phi(t,s)$ to 0 as $t-s \to \infty$ is sufficiently rapid, the lower bound s' of the integration in Eq. (A13) can be replaced by s, and we obtain

$$B_{21}(t,s) \simeq B_{22}(t,s)\int_s^t ds'\phi(s',s). \tag{A17}$$

With $f(t) = (\tilde{\eta}(t)/\tau, 0)^t$ and Eq. (A6), we obtain

$$\delta x_1(t) = B_{11}(t,t_0)\delta x_1(t_0) + B_{12}(t,t_0)\delta x_2(t_0) + \frac{1}{\tau}\int_{t_0}^t ds\tilde{\eta}(s)B_{11}(t,s), \tag{A18}$$

$$= \frac{1}{\tau}\int_{-\infty}^t ds\tilde{\eta}(s)B_{11}(t,s), \tag{A19}$$

where the limit $t_0 \to -\infty$ is taken, and

$$\langle \delta x_1(t)^2\rangle = \frac{1}{\tau^2}\int_{-\infty}^t\int_{-\infty}^t dsds' B_{11}(t,s)B_{11}(t,s')\langle\tilde{\eta}(s)\tilde{\eta}(s')\rangle, \tag{A20}$$

$$= \frac{\tilde{D}}{\tau^2}\int_{-\infty}^t dsB_{11}(t,s)^2, \tag{A21}$$

where $\tilde{D} \equiv (1-N^{-1})D$.

In order to obtain an approximate form for the variance $\langle \delta x_1(t)^2\rangle$, let us roughly evaluate $B_{11}(t,s)$ by the approximation $\phi(t,s) \sim e^{-\kappa(t-s)}$ with large κ, which leads to

$$\psi(t,s) \sim \frac{1-\phi(t,s)}{\tau\kappa}, \tag{A22}$$

$$B_{21}(t,s) \sim \frac{1-\phi(t,s)}{\kappa}B_{22}(t,s). \tag{A23}$$

For the variance in Eq. (A21), the three terms in

$$B_{11}^2 \simeq \phi^2 - 2\phi\psi B_{21} + \psi^2 B_{21}^2 \tag{A24}$$

give the contributions of the magnitudes of κ^{-1}, κ^{-3}, and κ^{-4}, respectively, thus we obtain

$$\langle \delta x_1(t)^2\rangle \simeq \frac{\tilde{D}}{\tau^2}\int_{-\infty}^t ds\phi(t,s)^2, \tag{A25}$$

$$= \frac{\tilde{D}}{\tau^2}\int_{-\infty}^t ds\exp\left[-\frac{2}{\tau}(w-1)(t-s) - \frac{2}{\tau}\int_s^t dt' X_1^2(t')\right]. \tag{A26}$$

If $(w-1)/\tau$ is sufficiently large, by replacing $X(t')$ by $X(t)$, we obtain

$$\langle \delta x_1(t)^2 \rangle \simeq \frac{\tilde{D}}{\tau^2} \int_{-\infty}^{t} ds \exp\left[-\frac{2}{\tau}(w - 1 + X_1^2(t))(t-s) \right], \tag{A27}$$

$$= \frac{(1-N^{-1})D}{2\tau(w-1+X_1^2)}. \tag{A28}$$

APPENDIX B: DISTRIBUTIONS OF $\delta x_1^{(i)}$ AND $(\delta x_1)^2$

In this section, we derive the distributions of $\delta x_1^{(i)}$ and $(\delta x_1)^2$. As shown in Eq. (A19) in Appendix A, $\delta x_1^{(i)}$ is expressed as

$$\delta x_1^{(i)} \simeq Z_i - \frac{1}{N}\sum_{k=1}^{N} Z_k, \tag{B1}$$

$$Z_i \equiv \frac{1}{\tau}\int_{-\infty}^{t} ds \eta^{(i)}(s) B_{11}(t,s), \tag{B2}$$

$$\langle \eta^{(i)}(s)\eta^{(j)}(s') \rangle = D\delta_{ij}\delta(s-s'). \tag{B3}$$

From the definition of the stochastic integral [41], Eq. (B2) is modified as

$$Z_i \simeq \frac{1}{\tau}\sum_{k=1}^{M} \frac{B_{11}(t,s_k) + B_{11}(t,s_{k+1})}{2}[\eta^{(i)}(s_{k+1}) - \eta^{(i)}(s_k)], \tag{B4}$$

$$= \sum_{k=1}^{M} a_k z_k, \tag{B5}$$

$$\tag{B6}$$

where

$$a_k \equiv \frac{B_{11}(t,s_k) + B_{11}(t,s_{k+1})}{2\tau}, \tag{B7}$$

$$z_k \equiv \eta^{(i)}(s_{k+1}) - \eta^{(i)}(s_k). \tag{B8}$$

Note that z_k is a random variable which follows a Gaussian distribution with the mean 0 and the variance $D\Delta t$ where $\Delta t \equiv s_{k+1} - s_k$. The distribution $P(Z,t)$ of Z_i is calculated as

$$P(Z;t) = \langle \delta(Z - Z_i) \rangle, \tag{B9}$$

$$\simeq \int \prod_{j=1}^{M} [dz_j P(z_j)] \, \delta\left(Z - \sum_{k=1}^{M} a_k z_k \right), \tag{B10}$$

$$\propto \int \prod_{j=1}^{M} dz_j \exp\left(-\frac{1}{2D\Delta t}\sum_{k=1}^{M} z_k^2 \right) \delta\left(Z - \sum_{k=1}^{M} a_k z_k \right), \tag{B11}$$

$$= \int \prod_{j=2}^{M} dz_j \exp\left[-\frac{1}{2D\Delta t}\left\{\sum_{k=2}^{M} z_k^2 + \frac{1}{a_1^2}\left(Z - \sum_{k=2}^{M} a_k z_k\right)^2\right\}\right], \tag{B12}$$

$$= \int \prod_{j=2}^{M} dz_j \exp\left[-\frac{1}{2D\Delta t}\left\{\frac{a_1^2+a_2^2}{a_1^2}\left(z_2 - \frac{a_2}{a_1^2+a_2^2}\left(Z - \sum_{k=3}^{M} a_k z_k\right)\right)^2\right\}\right]$$
$$\times \exp\left[-\frac{1}{2D\Delta t}\left\{\sum_{k=3}^{M} z_k^2 + \frac{1}{a_1^2+a_2^2}\left(Z - \sum_{k=3}^{M} a_k z_k\right)^2\right\}\right], \tag{B13}$$

$$\propto \int \prod_{j=3}^{M} dz_j \exp\left[-\frac{1}{2D\Delta t}\left\{\sum_{k=3}^{M} z_k^2 + \frac{1}{a_1^2+a_2^2}\left(Z - \sum_{k=3}^{M} a_k z_k\right)^2\right\}\right], \tag{B14}$$

$$\propto \cdots \propto \exp\left[-\frac{1}{2D\Delta t}\frac{Z^2}{\sum a_k^2}\right]. \tag{B15}$$

From the definition of a_k and Eq. (A21), $D\Delta t \sum a_k^2$ is written as

$$D\Delta t \sum_k a_k^2 \simeq \frac{D}{\tau^2}\int ds B_{11}(t,s)^2, \tag{B16}$$

$$\simeq \frac{\langle(\delta x_1^{(i)})^2\rangle}{1-N^{-1}}, \tag{B17}$$

$$\equiv \sigma_0^2, \tag{B18}$$

thus Z_i is Gaussian following

$$P(Z;t) \propto \exp\left(-\frac{Z^2}{2\sigma_0^2}\right) \tag{B19}$$

and statistically independent each other. The distribution $P_1(y;t)$ of $\delta x_1^{(i)} = Z_i - (1/N)\sum Z_k$ is calculated as

$$P_1(y;t) \simeq \int \prod_{j=1}^{N} [dZ_j P(Z_j;t)]\, \delta\left(y - Z_i + \frac{1}{N}\sum_{k=1}^{N} Z_k\right), \tag{B20}$$

$$\propto \exp\left(-\frac{y^2}{2\sigma_0^2(1-N^{-1})}\right), \tag{B21}$$

$$= \exp\left(-\frac{y^2}{2\langle(\delta x_1^{(i)})^2\rangle}\right). \tag{B22}$$

Thus it is concluded that $\delta x_1^{(i)}$ follows a Gaussian distribution with the mean 0 and the variance $\langle(\delta x_1^{(i)})^2\rangle$.

Next the distribution $P_2(y;t)$ of $(\delta x_1)^2 \equiv (1/N)\sum(\delta x_1^{(i)})^2$ is calculated as

$$P_2(y;t) = \langle\delta(y - (\delta x_1)^2)\rangle, \tag{B23}$$

$$= \left\langle \delta\left(y - \frac{1}{N}\sum_{i=1}^{N}(\delta x_1^{(i)})^2\right)\right\rangle, \tag{B24}$$

$$= \left\langle \delta \left(y - \frac{1}{N} \sum_{i=1}^{N} \left(Z_i - \frac{1}{N} \sum_{k=1}^{N} Z_k \right)^2 \right) \right\rangle, \tag{B25}$$

$$= \int \prod_{j=1}^{N} [dZ_j P(Z_j;t)] \delta \left(y - \frac{1}{N} \sum_{i=1}^{N} \left(Z_i - \frac{1}{N} \sum_{k=1}^{N} Z_k \right)^2 \right). \tag{B26}$$

Introducing cylindrical coordinates

$$h = \frac{1}{N} \sum_{i=1}^{N} Z_i, \tag{B27}$$

$$r = \sqrt{\frac{1}{N} \sum_{i=1}^{N} (Z_i - h)^2}, \tag{B28}$$

and $N-2$ angles, Eq. (B26) is calculated as

$$P_2(y;t) \propto \int dh dr \; r^{N-2} \delta(y - r^2) \exp\left(-\frac{N}{2\sigma_0^2} (r^2 + h^2) \right), \tag{B29}$$

$$\propto \int_0^\infty dr \; r^{N-2} \frac{1}{2r} \delta(r - \sqrt{y}) \exp\left(-\frac{N}{2\sigma_0^2} r^2 \right), \tag{B30}$$

$$\propto y^{(N-3)/2} \exp\left(-\frac{N}{2\sigma_0^2} y \right), \tag{B31}$$

$$= \exp\left[-\frac{N}{2\sigma_0^2} \left(y - \frac{N-3}{N} \sigma_0^2 \log y \right) \right]. \tag{B32}$$

With this distribution, the mean and the variance of $(\delta x_1)^2$ are calculated as

$$\langle y \rangle = (1 - N^{-1}) \sigma_0^2 = \langle (\delta x_1^{(i)})^2 \rangle, \tag{B33}$$

$$\langle (y - \langle y \rangle)^2 \rangle = \frac{2}{N-1} \langle (\delta x_1^{(i)})^2 \rangle^2. \tag{B34}$$

From Eqs. (B33) and (B34), the approximation $(\delta x_1)^2 \simeq \langle (\delta x_1^{(i)})^2 \rangle$ is justified for large N.

---

[1] F. Moss, D. Pierson, and D. O'Gorman, Int. J. Bif. and Chaos **4**, 1383 (1994).

[2] M. I. Dykman, D. G. Luchinsky, R. Mannella, P. V. E. McClintock, N. D. Stein, and N. G. Stocks, Nuovo Cimento D **17**, 661 (1995).

[3] L. Gammaitoni, P. Hänggi, P. Jung, and F. Marchesoni, Rev. Mod. Phys. **70**, 223 (1998).

[4] K. Wiesenfeld and F. Jaramillo, CHAOS **8**, 539 (1998).

[5] C. U. M. Smith, *Biology of Sensory Systems* (John Wiley & Sons Ltd, West Sussex, England, 2000).

[6] L. J. DeFelice and A. Isaac, J. Stat. Phys. **70**, 339 (1992).

[7] S. W. Kuffler, J. G. Nicholls, and A. R. Martin, *From Neuron to Brain* (Sinauer Associates Inc. Publishers, Sunderland, Massachusetts, 1984).

[8] C. Rosenmund, J. D. Clements, and G. L. Westbrook, Science **262**, 754 (1993).

[9] N. A. Hessler, A. M. Shirke, and R. Malinow, Nature (London) **366**, 569 (1993).

[10] M. N. Shadlen and W. T. Newsome, Curr. Opin. in Neurobiol. **4**, 569 (1994).

[11] G. Mato, Phys. Rev. E **58**, 876 (1998).

[12] G. Mato, Phys. Rev. E **59**, 3339 (1999).

[13] Y. Sakumura and K. Aihara, in *Proceedings of the Fifth International Conference on Neural Information Processing*, edited by S. Usui and T. Omori (Ohmsha, Tokyo, 1998), p. 951.

[14] J. Feng and B. Tirozzi, Phys. Rev. E **61**, 4207 (2000).

[15] H. Hayashi, S. Ishizuka, M. Ohta, and K. Hirakawa, Phys. Lett. A **88**, 435 (1982).

[16] G. Matsumoto, K. Aihara, M. Ichikawa, and A. Tasaki, J. Theor. Neurobiol. **3**, 1 (1984).

[17] W. J. Freeman, Biol. Cybern. **56**, 139 (1987).

[18] A. R. Bulsara, S. B. Lowen, and C. D. Rees, Phys. Rev. E **49**, 4989 (1994).

[19] A. R. Bulsara, T. C. Elston, C. R. Doering, S. B. Lowen, and K. Lindenberg, Phys. Rev. E **53**, 3958 (1996).

[20] T. Shimokawa, K. Pakdaman, and S. Sato, Phys. Rev. E **59**, 3427 (1999).

[21] A. Longtin, J. Stat. Phys. **70**, 309 (1993).

[22] K. Wiesenfeld, D. Pierson, E. Pantazelou, C. Dames, and F. Moss, Phys. Rev. Lett. **72**, 2125 (1994).

[23] A. Longtin and D. R. Chialvo, Phys. Rev. Lett. **81**, 4012 (1998).

[24] S. Lee and S. Kim, Phys. Rev. E **60**, 826 (1999).

[25] J. K. Douglass, L. Wilkens, E. Pantazelou, and F. Moss, Nature (London) **365**, 337 (1993).

[26] X. Pei, L. A. Wilkens, and F. Moss, J. Neurophysiol. **76**, 3002 (1996).

[27] B. J. Gluckman, T. I. Netoff, E. J. Neel, W. L. Ditto, M. L. Spano, and S. J. Schiff, Phys. Rev. Lett. **77**, 4098 (1996).

[28] B. J. Gluckman, P. So, T. I. Netoff, M. L. Spano, and S. J. Schiff, CHAOS **8**, 588 (1998).

[29] D. Nozaki, D. J. Mar, P. Grigg, and J. J. Collins, Phys. Rev. Lett. **82**, 2402 (1999).

[30] F. Moss and X. Pei, Nature (London) **376**, 211 (1995).

[31] J. J. Collins, C. C. Chow, and T. T. Imhoff, Nature (London) **376**, 236 (1995).

[32] T. Shimokawa, A. Rogel, K. Pakdaman, and S. Sato, Phys. Rev. E **59**, 3461 (1999).

[33] S. Tanabe, S. Sato, and K. Pakdaman, Phys. Rev. E **60**, 7235 (1999).

[34] T. Kanamaru, T. Horita, and Y. Okabe, Phys. Lett. A **255**, 23 (1999).

[35] T. Kanamaru and Y. Okabe, BioSystems **58**, 101 (2000).

[36] M. Löcher, D. Cigna, E. R. Hunt, G. A. Johnson, F. Marchesoni, L. Gammaitoni, M. E. Inchiosa, and A. R. Bulsara, CHAOS **8**, 604 (1998).

[37] J. F. Lindner, B. K. Meadows, W. L. Ditto, M. E. Inchiosa, and A. R. Bulsara, Phys. Rev. Lett. **75**, 3 (1995).

[38] M. Löcher, G. A. Johnson, and E. R. Hunt, Phys. Rev. Lett. **77**, 4698 (1996).

[39] B. Hu and C. Zhou, Phys. Rev. E **61**, R1001 (2000).

[40] G. Palm, A. M. H. J. Aertsen, and G. L. Gerstein, Biol. Cybern. **59**, 1 (1988).

[41] C. W. Gardiner, *Handbook of Stochastic Methods* (Springer-Verlag, Berlin, 1985).